A Model for Shrinkage of a Spherical Void in the Center of a Grain: Influence of Lattice Diffusion

Jun Sun

(Submitted 4 January 2002)

A model is presented to describe a spherical void shrinkage at the center of a quasi-spherical grain dominated by lattice self-diffusion. The model is based on the difference in chemical potential between the spherical void surface and the grain boundary interface. The quantitative calculations for pure iron predicted that only small, micron-sized spherical voids could be wholly healed within hours at high temperature. The spherical void shrinkage process can be greatly promoted with an increase in temperature, which depends strongly on crystal lattices, particularly the initial radius of the spherical void and the grain size. The time to eliminate a spherical void with an identical radius within grains is close to that for grain boundaries, while different shrinkage processes were undergone, at fixed temperatures, and related to spherical void size, void spacing, and the grain size.

Keywords chemical potential, grain size, lattice diffusion, shrinkage, spherical void

1. Introduction

High-temperature internal crack healing and microstructurally similar processes have been the subject of considerable interest and study for many years.[1-6] The diffusive healing processes that occur at elevated temperature can reduce the deleterious effects of cracks on strength, allowing partial or complete recovery of strength in such cracked materials as ceramic and its composites.[1-6] In addition, the morphological changes during crack healing, sintering, and diffusion bonding have many similarities.[7-11] Similar transport mechanisms also may control or affect these three processes. Thus, investigations into internal crack healing may also contribute to an improved fundamental understanding of sintering and diffusion bonding.

Most studies of internal crack healing have revealed several geometrically distinct stages to the process.[12-16] The initial stage is characterized by crack tip regression and blunting, i.e., surface tension would cause the edges of the crack to recede toward the center and grow in girth. The second stage of crack healing is accompanied by the formation of cylindrical pore channels, which results in a doughnut-shaped rim spanned by the remainder of the crack. Finally, the cylindrical pore channels that are formed are subject to Rayleigh instabilities, leading to the formation of discrete spherical voids both on grain boundaries and within grains.

In contrast, for metals, the spherical voids can be directly introduced mainly on grain boundaries (and a few within grains) by either creep or fatigue at high temperature.[17-20] However, during the high-temperature creep and fatigue at atmospheric environment, gas diffused into the voids tends to build up an internal pressure inside the voids to balance the surface tension forces, which tend to close the voids and then retard the void shrinkage. In the present study, only a gas-free spherical void was treated.

Alternatively, annealing at high temperature for crack healing and void shrinkage could cause grain growth and grain boundary migration as atoms detach from one grain and join another, which could also isolate many spherical voids initially on grain boundaries stranded inside the grains.[17,20,21] That is, the voids separate from the grain boundaries. After being trapped inside the grains, the spherical voids can only be eliminated by lattice diffusion, which is a much slower process than grain boundary diffusion.[21] Consequently, the separation leads to a porous, coarse-grained ceramic. Therefore, it is traditionally believed that it is difficult to produce a dense, fine-grained ceramic by totally healing the voids within grains through lattice diffusion, even when an external hydrostatic pressure is applied.

The formation of isolated spherical voids is, generally, referred to as completion of the crack healing for the porous materials, such as ceramics, because the spherical voids represent relatively stable void shapes with the smallest surface areas, when total volumes of initial cracks remain constant.[3,22,23] More importantly, it is believed that the recovery of strength in ceramics results not from continued shrinkage of small spherical voids, but rather from continued pinching off of the remaining cylindrical channel voids.[2,3] Similarly, for diffusion bonding, the whole bonding process was also regarded as the changes from initial void shapes to circular profiles on the bonding interface.[10,24,25] However, for metals, the recovery of creep ductility properties has been positively attributed to the shrinkage of spherical voids on grain boundaries, relative to the small tendency of voids to shrink within grains.[17] Therefore, for close-grained materials, or metals, it is expected that the spherical voids should be eliminated as the final stage of the crack healing, whether on grain boundaries or within grains. Until now, to the author's knowledge, little attention has been devoted to the spherical void shrinkage within grains.

Jun Sun, State Key Laboratory for Mechanical Behavior of Materials, School of Materials Science and Engineering, Xi'an Jiaotong University, Xi'an 710049, People's Republic of China. Contact e-mail: junsun@xjtu.edu.cn.

In the last two decades, many efforts have been made to investigate void shrinkage on the planar bonding interface or the planar grain boundary interface,[26] under surface or interface self-diffusion, or both. Some void shrinkage models[27-29] were developed from powder sintering models,[30,31] and others[10,32] were derived from void growth models,[33-36] including that of spherical voids,[37] where an improper boundary condition was used[24] under tensile creep, treating void shrinkage as negative void growth. Note, however, that all of the models can only be used to describe the process of void shrinkage on bonding interfaces or grain boundaries, but not that within grains.

In fact, the spherical void has an intrinsic tendency to shrink under the action of surface tension forces, regardless of whether they are on grain boundaries or within grains, although it was believed that the shrinkage rates of spherical voids within grains were much lower than those on grain boundaries.[17,20,21] In other words, the void shrinkage also can be operated within grains because of the difference in chemical potential between the spherical void surface and the quasi-spherical grain boundary interface surrounding the shrinking void and following mass transfer driven by the gradient of the chemical potential. Moreover, spherical void shrinkage within a grain, if adopted as a final stage of the whole internal crack healing, might be a rate-controlling step because it is dominated by a lattice self-diffusion, which is much slower than that by either surface or interface diffusions. Along this line, the work reported here presents a model to describe the void shrinkage in the center of the quasi-spherical grain dominated by lattice self-diffusion of atoms. The model is based on the difference in chemical potential between atoms on the spherical void surface and quasi-spherical grain boundary interface.

2. Background

For a curved surface, an excess chemical potential is usually expressed by

$$\Delta\mu = \mu - \mu_0 = \gamma\Omega K \qquad \text{(Eq 1)}$$

where μ and μ_0 is the chemical potential of a species on a curved and a planar surface, respectively; $\gamma\Omega K$ is the excess chemical potential produced by the present of the surface curvatures; γ is the surface tension (assumed to be isotropic here); Ω is the atomic volume; and $K = 1/R_1 + 1/R_2$ is the mean curvature of the surface at the point of interest (where R_1 and R_2 are the principal radii of the curvature).

For diffusion-controlled capillary instability of rod morphologies,[12,38] the excess chemical potential induced by the surface curvature has always referred to a positive value, regardless of the difference between a convex surface and a concave surface. Perhaps the absence of the distinction is acceptable in the investigations into the undulation of the rod along its longitudinal direction. However, the excess chemical potential should be identified as positive for a convex surface and a negative for a concave surface where both surface profiles have to be involved, as indirectly suggested in related research.[10,39-44]

In general, direct cylinderization always occurs for a plate and a hole not having internal boundaries, during which the plate's transverse cross section evolves into a circle even for rectangular- and "I"-shaped plates.[45,46] Similarly, an equilibrium circular cross-sectional shape also would be approached as a result of diffusion along the curved surface of a plate and a hole with an elliptical cross-sectional shape, as shown in Fig. 1. Clearly, the variation of the excess chemical potential on the curved surface with radius R for a plate is different from that for a hole. That is, the excess chemical potential, $\Delta\mu = \mu_R - \mu_0$, becomes either more positive (higher) or negative (lower) with decreasing radius R for both plate and hole surfaces. Therefore, the atoms would diffuse along the surface from B to A for the plate and from D to C for the hole because $\mu_R(B) > \mu_R(A)$ for a convex surface and $\mu_R(D) > \mu_R(C)$ for a concave surface, respectively. Consequently, the transverse cross-sectional shape of both a plate and a hole approaches the equilibrium circular cross-sectional shape to reduce the total surfaces at fixed volumes. Otherwise, the shape evolution process will be applicable for only one case, either a convex surface or a concave surface, if the excess chemical potential is not identified as positive or negative individually. Therefore, Eq 1 can be rewritten as

$$\Delta\mu = \mu - \mu_0 = \pm\gamma\Omega K \qquad \text{(Eq 1-1)}$$

where the positive or negative value corresponds to a convex (protruding) or a concave surface, respectively.

In a similar way, a rod, or a plate-shaped particle and a void, which have three-dimensional sizes near to each other, is susceptible to direct spheroidization as a result of a curvature-induced self-diffusion process. Both the particle and the void evolve into a spherical shape with reduction in total surface area, during which the morphology change is completed.

On the other hand, the known "Ostwald ripening" of precipitates and, similarly, either growth or shrinkage of spherical voids with different radii controlled by lattice diffusion could also be described based on the understanding mentioned above. We start with the simplest system consisting of two spherical

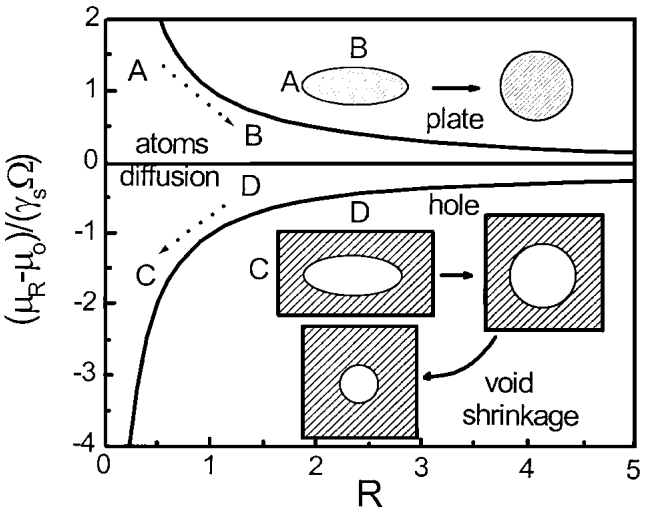

Fig. 1 Cylinderization of an elliptical plate and an elliptical hole and shrinkage of a spherical void

precipitates (convex surfaces) of different radii, r_1 and r_2 ($r_1 < r_2$). In this section, where $\mu(r_1) > \mu(r_2)$ μ, there will be a diffusive flux of atoms of the precipitates from 1 to 2, which results in the shrinkage of the small precipitate and the growth of the larger, leaving only one somewhat larger precipitate in the system. The same phenomenon also occurs in the sintering of rows of spherical particles, where smaller particles disappear and larger particles grow.[47] We next consider a system consisting of two spherical voids (concave surfaces) of different radii, r_1 and r_2 ($r_1 < r_2$). In this case, where $\mu(r_1) < \mu(r_2)$, the atoms will diffuse from the surface of void 2 to that of void 1, which will lead to the reduction and enlargement in the sizes of the smaller void and larger void, respectively. During the processes, the total surface area is reduced by the growth of larger particles or voids at the expense of the shrinkage of smaller particles or voids, and their eventual disappearance, whereas the total volume is invariant.

Note that the curvature-induced diffusion process and resultant morphology change described are dominated by surface self-diffusion when the total volume of the system remains constant. The formation of the sphere is generally considered to be a complete finish of the shape evolution because it has the most stable morphology and the lowest system free energy relative to any other shapes. However, a new diffusion process of atoms will occur between the spherical void surface and the adjacent grain boundary interface or other surface, where a source of or a sink for vacancies or atoms is because of the difference in chemical potential between them. Then the size of the spherical void could vary by the new self-diffusion, while the void retains its invariant spherical shape throughout the change in its size. The process should be dominated by either grain boundary diffusion for voids on the grain boundaries or lattice diffusion for voids within grains, and faster surface diffusion would keep the spherical void shape unchanged during the process. As also indicated in Fig. 1, the total surface area of the void and the free energy of the system will be reduced with decreasing void volume.

Therefore, it is reasonable to present a model to describe the shrinkage of a spherical void in the center of an equiaxial grain dominated by lattice self-diffusion of atoms at high temperature, on the basis of the difference in chemical potential between atoms on the spherical void surface and equiaxial grain boundary interface.

3. Model

As stated above, some separated spherical voids were left in a polycrystalline solid, both on a grain boundary and within a grain, as a result of the healing of an internal penny-shaped microcrack in high-temperature annealing. Finger-like channels emerged from the morphological changes of the crack and the formation of many small voids. On the other hand, annealing at high temperature can also cause grain growth, which will isolate many spherical voids initially on grain boundaries stranded inside the grains.[17,20,21] However, only shrinkage of a spherical void within a grain will be treated in the present paper.

A schematic model is depicted in Fig. 2. For a polycrystalline solid, an isolated spherical void of radius ρ is embedded in

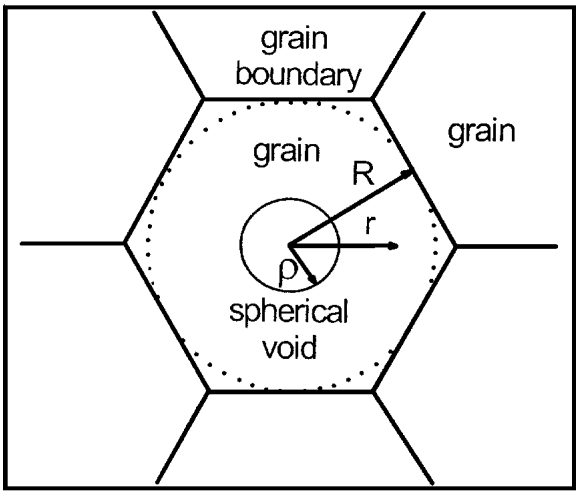

Fig. 2 A model with a spherical void of a radius ρ embedded in the center of a quasi-spherical grain of radius R; r is the distance to the center of the void

the center of an equiaxial grain, approximately spherical grain of radius R (or the distance from the center of the void to the grain boundary interface), and r is the distance to the center of the void. On the basis of the above approach, it is reasonable to express the excess chemical potentials of the concave void surface,[10,39-44] and particularly the convex grain boundary interface, respectively, as follows

$$\Delta\mu_\rho = -2\gamma_s\Omega/\rho \quad \text{(Eq 2)}$$

and

$$\Delta\mu_R = 2\gamma_{gb}\Omega/R \quad \text{(Eq 3)}$$

where γ_s and γ_{gb} are surface tension and grain boundary energy of the polycrystalline solid, respectively.

The term on the right-hand side of Eq 3 arises from the assumed convex grain boundary, which does not exist in modeling of either the void shrinkage or the void growth on grain boundary interface, where only a planar interface is involved.

Identical to those on a grain boundary interface and a surface, the atom flux proportional to the gradient of an excess chemical potential along the radial direction from the grain boundary interface to the void surface is also expressed by[40,41,49]

$$J = -(D_l/kT\Omega)\nabla\Delta\mu \quad \text{(Eq 4)}$$

where D_l is the lattice self-diffusion coefficient (assumed to be isotropic), k is the Boltzmann constant, and T is the absolute temperature.

D is described as $D_0 \exp(-Q/RT)$, where D_0 is the frequency factor, R is the gas constant, and Q is the activation energy for self-diffusion. D for the surface and bulk (through the lattice) self-diffusion are denoted by the subscripts s and l, respectively.

Void shrinkage or growth occurs from the ability of the

grain boundary to behave as a perfect and inexhaustible source of or sink for either vacancies or atoms, depending on the whether the grain boundary interface has either higher or lower excess chemical potential than that of the spherical void surface. In the steady state, when stress redistribution is completed, vacancy elimination or formation must occur at a constant rate over the entire boundary area.[24,37] For lattice self-diffusion, steady state is obtained by

$$div.J = \beta \qquad \text{(Eq 5)}$$

where β is the number of atoms removed per unit time and unit volume of the grain boundary interface through the grain lattice between the grain boundary interface and the void surface, where there is no mass accumulation or production inside the grain lattice and the source of atomic flux is purely the grain boundary interface area.

Substituting Eq 4 in Eq 5, we obtain the differential equation

$$\nabla^2\Delta\mu + (\beta kT\Omega/D_l) = 0 \qquad \text{(Eq 6)}$$

Assuming spherical symmetry in the variation of the excess chemical potential with the radial direction between the void surface and the grain boundary interface, the appropriate solution giving the distribution of chemical potential with the radial coordinate r is

$$\Delta\mu = -(\beta kT\Omega/6D_l)r^2 + B + C/r \qquad \text{(Eq 7)}$$

or

$$\Delta\mu = Ar^2 + B + C/r \qquad \text{(Eq 7-1)}$$

where A, B, and C are constants to be determined.

Solving the differential equation for $\Delta\mu$, subject to the boundary conditions as given by Eq 2 and 3, and $\partial\Delta\mu/\partial r_{r=R} = 0$, which determines either generating or vanishing atomic flux at the grain boundary, respectively, for the shrinkage[24] or the expansion[37] of the spherical void, we obtain $\Delta\mu$ at any location in the grain with a radius of $r(\rho \le r \le R)$ expressed by

$$\Delta\mu = \frac{(2\gamma_{gb}/R + 2\gamma_s/\rho)\Omega}{(3R^2 - \rho^2 - 2R^3/\rho)}\left[r^2 - \rho^2 + 2R^3\left(\frac{1}{r} - \frac{1}{\rho}\right)\right] - \frac{2\gamma_s\Omega}{\rho} + P\Omega \qquad \text{(Eq 8)}$$

The variation of excess chemical potential with distance from the center of the void, r, is shown in Fig. 3. The excess chemical potential decreases gradually from the grain boundary, $r = R$, to the void surface, $r = \rho$, and the larger the ratio of ρ to R, the lower the gradient. The atoms are driven by the gradient of the excess chemical potential to diffuse from the grain boundary interface into the void surface along the radial direction, which would lead to the spherical void shrinking and finally vanishing.

However, as expected, the gradient of the excess chemical potential remains unchanged with an increase in hydrostatic pressure, P, which elevates the excess chemical potential with an identical magnitude on the grain lattices between the spherical grain boundary interface and the spherical void surface, as indicated in Fig. 3. The result suggested that the spherical void shrinkage in a grain was independent from the hydrostatic pressure normally acting on the grain boundary interface. The prediction is in good agreement with the experimental observations on the spherical void shrinkage in copper under hydrostatic pressure.[17,20] The experimental examinations showed that, for spherical voids on the grain boundaries, the shrinkage process was accelerated by an increase in hydrostatic pressure. However, for spherical voids situated within the grains, no tendency to shrink was observed under the same hydrostatic annealing conditions.

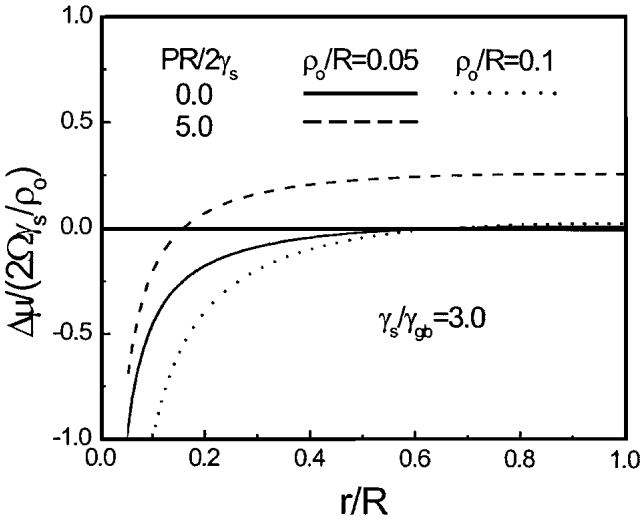

Fig. 3 The radial distribution of chemical potential from void surface to grain boundary interface

The plots also revealed that the gradient of the excess chemical potential gradually vanishes as it moves away from the spherical void surface, within the grain lattice of $R \ge r \ge (R - \rho)/2$. On the other hand, the plots also indicated that the excess chemical potential of the convex grain boundary as assumed, approaches zero over the grain lattice close to the grain boundary interface, compared with that of the spherical void surface where $\gamma_s\Omega/\rho$ is much greater than $\gamma_{gb}\Omega/R$. In other words, the chemical potential of the convex grain boundary is identical to that of the planar interface and independent from both the curvature of the grain boundary interface and the geometric singularities resulting from the multigrain junctions. That is, the second term on the right-hand side of Eq 3 presented by the convex grain boundary, i.e., the almost zero contribution of the grain boundary curvature to the excess chemical potential, can be generally omitted.[24,37] Then one has $\Delta\mu_R = 0$ in Eq 3, relative to $\gamma_s\Omega/\rho$ in the case without the external hydrostatic pressure. The result implies that it is not critical to assume either a spherical or planar grain boundary interface for the spherical void shrinkage in the grain. The planar grain boundary interfaces with multigrain junctions, usually observed in crystals, can be reasonably treated in the model. Furthermore, it should be pointed out that the physical meaning of the radius of the grain, R, is actually the distance from the center of the spherical void to the flat or curved grain boundary interface surrounded.

The rate of the void shrinkage is determined by the gradient of chemical potential evaluated at the void surface, and then the diffusion flux is given by

$$J = \frac{D_l}{kT\Omega}\left(\frac{\partial \Delta\mu}{\partial r}\right)_{r=\rho} = -\frac{2D(2\gamma_{gb}/R + 2\gamma_s/\rho)}{kT(3R^2 - \rho^2 - 2R^3/\rho)}\left(\rho - \frac{R^3}{\rho^2}\right) \quad \text{(Eq 9)}$$

If the void retains its spherical shape by surface diffusion, we have the rate of void shrinkage

$$\frac{d\rho}{dt} = -\frac{2D_l\Omega(2\gamma_{gb}/R + 2\gamma_s/\rho)}{kT\,(3R^2 - \rho^2 - 2R^3/\rho)}\left(\rho - \frac{R^3}{\rho^2}\right) \quad \text{(Eq 10)}$$

which is independent of external hydrostatic pressure. On integrating from ρ_0 (initial radius of the void) to $a_0/2$ (atomic radius), assuming $\rho_0 >> a_0$ or $a_0/2R \approx 0$, and ignoring growth of the grain, we obtain

$$t_0(s) = -\frac{kTR^3}{4D_l\gamma_s\Omega}\int_0^x \frac{bx^3\,(3x - x^3 - 2)}{(x+b)(1-x^4)}dx \quad \text{(Eq 11)}$$

where $x = \rho_0/R$, and $b = \gamma_s/\gamma_{gb}$. However, no analytical solution for $t_0(s)$ can be rationally given by the x integral of Eq 11. As another choice, numerical calculations indicate that Eq 11 can be exactly replaced with the relative errors below 1% within the range of $0 \le \rho_0/R \le 0.4$ by

$$t_0(s) = -\frac{kTR^3}{4D_l\gamma_s\Omega}\int_0^x \frac{bx^3\,(3x - x^3 - 2)}{(x+b)}dx \quad \text{(Eq 11-1)}$$

$t_0(s)$ is given by

$$t_0(s) = -\frac{kTR^3b}{4D_l\gamma_s\Omega}\left\{(1+b)^2\left[b^2(b-2)\left(\frac{\rho_0}{R}\right) + \frac{b}{2}(2-b)\left(\frac{\rho_0}{R}\right)^2 + \frac{1}{3}(b-2)\left(\frac{\rho_0}{R}\right)^3\right] + \frac{1}{4}(3-b^2)\left(\frac{\rho_0}{R}\right)^4 + \frac{b}{5}\left(\frac{\rho_0}{R}\right)^5 - \frac{1}{6}\left(\frac{\rho_0}{R}\right)^6 + b^3\,(2 + 3b - b^3)\ln\left(1 + \frac{\rho_0}{bR}\right)\right\} \quad \text{(Eq 12)}$$

The time, $t_0(s)$, to totally heal the void of initial radius ρ_0/R, is enhanced monotonically with an increase in ρ_0/R, as demonstrated in Fig. 4, which seems insensitive to the ratio of surface tension to interface (grain boundary) energy, γ_s/γ_{gb}, particularly for small ρ_0/R. For an identical ρ_0/R, the larger the grain size, R, the shorter the total healing time, $t_0(s)$.

4. Predictions for Pure Iron

It is well known that the lattice-diffusion of metals is strongly dependent on their crystal lattices, temperature, and pressure. Pure iron is selected as the objective with body-centered cubic (bcc) and face-centered cubic (fcc) lattices of transformation temperature, $\alpha - Fe \leftrightarrow \gamma - Fe$, 1185 K, and annealing temperatures of α – Fe, 973, 1073, and 1173 K; and 1200, 1300, and 1400 K for γ – Fe. The total time, $t_0(h)$, to heal a spherical void of radius ρ_0 is predicted by Eq 12, using the following parameters: Boltzmann constant $k = 1.38 \times 10^{-23}$ $J \neq K$ and gas constant $R = 8.31$ J/mol · K, and others given in Table 1.

In the present study, the shrinkage of the spherical voids was investigated within a range of a grain radius R from 20 to 100 μm, which is usually present in pure iron.

4.1 Effects of Crystal Lattice and Temperature

Figure 5 gives the variation of the total healing time, $t_0(h)$, with initial radius of spherical voids, ρ_0, within a grain of radius R = 20 to 100 μm at transformation temperature of 1185 K, for α – Fe and γ – Fe, respectively, which increases monotonically and linearly as ρ_0 at the scale of some hundreds of hours. However, the time to heal voids with identical ρ_0 for α – Fe and γ – Fe depends highly on the crystal lattices. Obviously the longer times, $t_0(h)$, are needed for γ – Fe than those for α – Fe at the same temperature of 1185 K because γ – Fe has lower lattice diffusion constants, and, in particular, higher activation energy of self-diffusion.

As presented in Fig. 6, the times, $t_0(h)$, are remarkably decreased initially and then continue to decrease gradually as temperature increases from 1000 to 1185 K in α – Fe, and from 1185 to 1400 K in γ – Fe, respectively, for a spherical void of

Table 1 Diffusion Parameters for Pure Iron

Parameters	α – Fe	γ – Fe
γ_s = J/m^2[48]	2.2	2.2
γ_{gb} = J/m^2[48]	0.8	0.8
a_0(m) × 10^{-10}	2.48	2.58
D_{os} (m^2/s)[35]	10	0.4
D_{ol} (m^2/s)[48]	1.9×10^{-4}	1.8×10^{-5}
Q_s (KJ/mol)[35]	233.52	205.8
Q_1 (KJ/mol)[48]	239	270

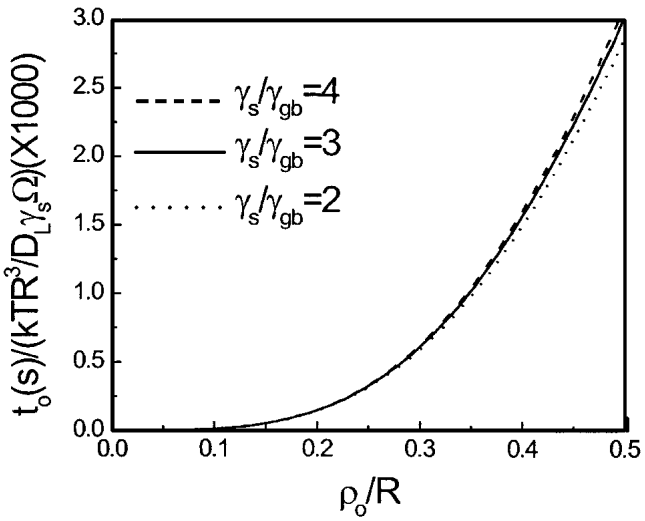

Fig. 4 The normalized time to heal a spherical void with an initial radius of ρ_0/R

radius $\rho_0 = 1$ μm, with grain radii of $R = 20$ and 100 μm. In addition, the gaps in the times, $t_0(h)$, resulting from the two values of R, are almost independent from increasing temperature. The spherical void shrinkage is accelerated with an increase in temperature by an exponential increase of the diffusion coefficient. For example, the times spent for γ – Fe at 1200 and 1400 K only correspond to those for α – Fe at 1000 and 1100 K, respectively, for a spherical void of radius $\rho_0 = 1$ μm within a grain of $R = 100$ μm. Fortunately, the times, $t_0(h)$, could be much reduced by annealing at a temperature higher than 1500 K for γ – Fe. Certainly, the larger the grain size, the less time will be needed, which will be discussed below.

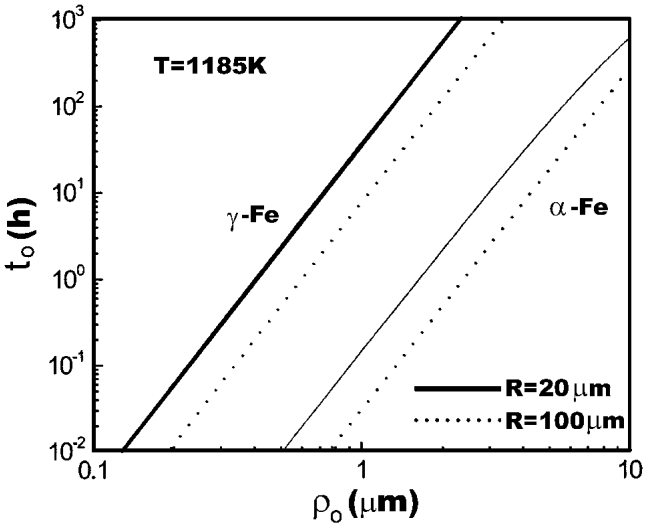

Fig. 5 The variations of healing time with the initial radii of spherical voids for α – Fe and γ – Fe with different grain radii at the transformation temperature

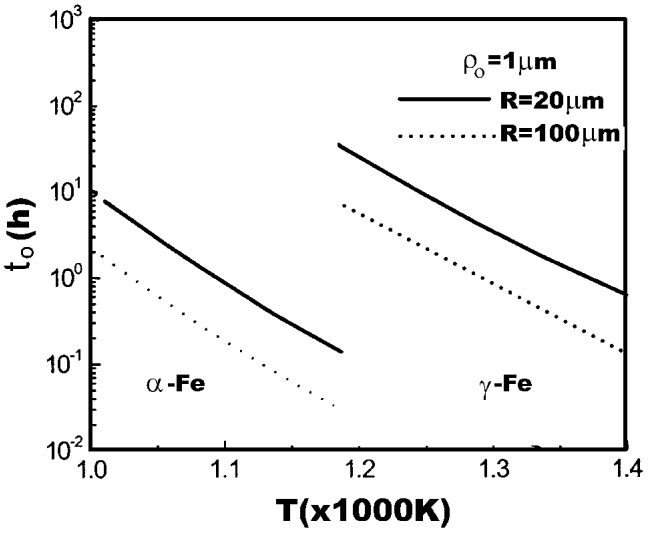

Fig. 6 The healing time as a function of temperature for a spherical void with an initial radius of $\rho_0 = 1$ μm in α – Fe with grain radii of $R = 20$ and 100 μm

4.2 Dependencies on Grain Sizes

Figure 7 shows the linear dependencies of the times, $t_0(h)$, on grain sizes for spherical voids, or the distance from the void center, with various radii of ρ_0 in α – Fe healed at a temperature of 973 K. The healing time is approximately inversely proportional to the grain sizes, $t_0 \propto 1/R$; i.e., the increased grain sizes lead to the shorter times to be expended for an identical ρ_0. This means that many more atoms were activated and gathered to diffuse from an enlarged grain boundary interface around the spherical void as the grain size increased, which raised the local chemical potential (particularly its gradient near to the void surface) and promoted the shrinkage of the void, as shown in Fig. 4. In another words, many more lattice sites were available on the enlarged grain boundary interface for the precipitation of vacancies diffused from the spherical void surface with an increase in grain sizes.

4.3 Time to Heal a Spherical Void with Radius of ρ_0

The times, $t_0(h)$, needed to heal a spherical void with a radius of ρ_0 are displayed in Fig. 8 and 9, and Table 2 for both α – Fe and γ – Fe in a large scale of grain sizes from 20 to 100 μm at temperatures selected, which exhibit linear relationships with similar slopes of $n = 4$, i.e., $t_0(h) \propto \rho_0^4$, regardless of the crystal lattices, grain sizes, and temperatures. The plots exhibit similar grain size and temperature dependencies of the healing times, $t_0(h)$, for spherical voids with various radii of ρ_0, as given above.

4.4 Comparison with Spherical Void Shrinkage on a Grain Boundary

Figure 10 gives temperature dependencies of the time to eliminate a spherical void with a radius of $\rho_0 = 1$ μm within grains of radii $R = 20$ and 100 μm, together with those of half-void spacing of $b = 2$ and 10 μm on a grain boundary for α – Fe.[50] The plots present stronger temperature dependencies

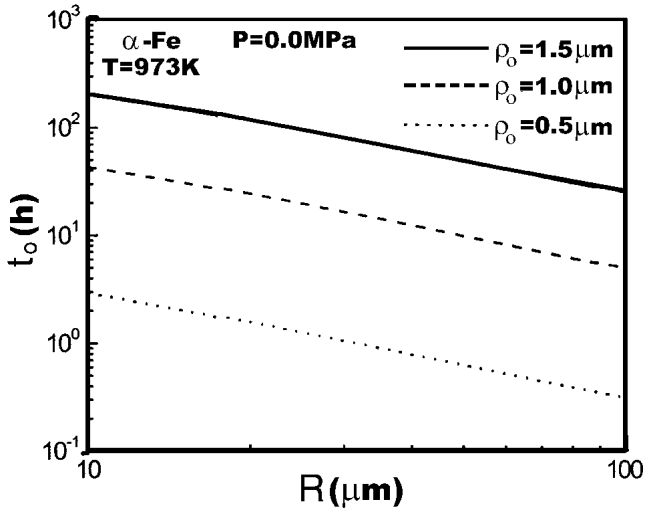

Fig. 7 The linear dependencies of healing time on grain sizes for spherical voids with various initial radii in α – Fe at a temperature of 973 K

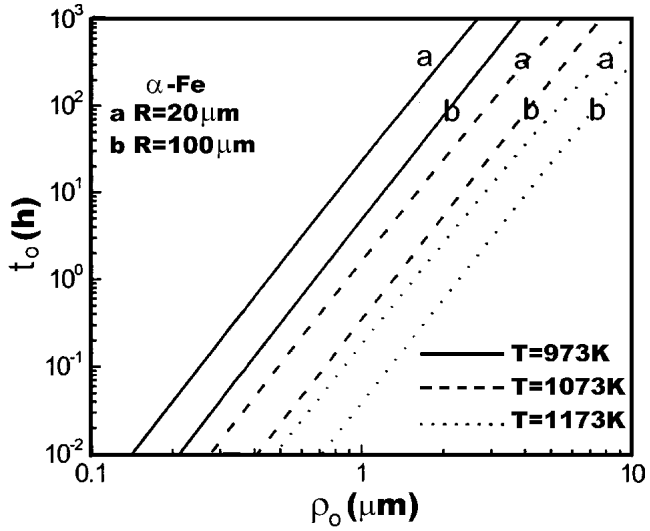

Fig. 8 The healing time linearly related to initial radii of spherical voids within grains of radii **(a)** R = 20 μm and **(b)** R = 100 μm in α – Fe at temperatures of 973, 1073, and 1173 K

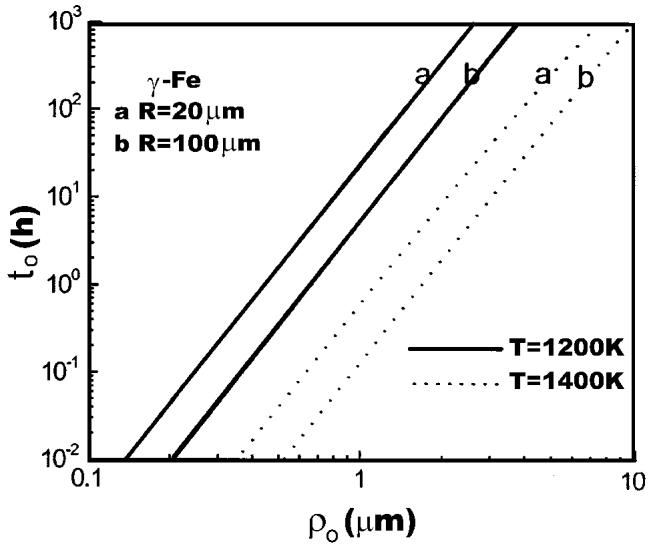

Fig. 9 The healing time linearly related to initial radii of spherical voids within grains of radii **(a)** R = 20 μm and **(b)** R = 100 μm in γ – Fe at temperatures of 1200, 1300, and 1400 K

for the former than those for the latter; the result is that the two groups of curves have an overlapped zone at 900-1000 K and gradually separate as the temperature increases. The gaps in the times, $t_0(h)$, resulting from the two values of either R or b, are almost independent from increasing temperature, respectively.

Generally, it seems that the times to heal voids with an identical radius within grains are not longer than in those on grain boundary interfaces at fixed annealing temperature for α – Fe, which differs apparently from the results in copper.[17,20] Of course, the mutual relation is highly dependent on the crystal lattices with a different ratio of diffusion coefficients, temperature, and the spherical void sizes (in particular, the void spacing on the grain boundary and the grain sizes), and cannot be confirmed simply.

Figure 11 illustrates the comparison of the shrinkage process of a spherical void of an initial radius ρ_0 = 1 μm relative to annealing time within a grain radius of R = 100 μm with that on a grain boundary of half-void spacing b = 2 μm[50] at a temperature of 973 K, both of which reduce its size with the annealing. It is interesting, however, that the shrinkage of spherical voids undergoes different sequences, the plots of which exhibit a remarkable decrease initially and then a gradual decrease for the spherical void on a grain boundary and inverse changes for the shrinkage process of an intragranular spherical void with annealing time. That is, for a spherical void of same radius within grains, the shrinkage rate is lower initially and higher finally than that on grain boundaries with annealing time at fixed temperature, whereas the total times for the voids to vanish are comparable to each other. Similar reversing tendencies in spherical void shrinking kinetics have been presented in the experimental observations of copper.[17,20] It was indicated that the rate of density increase of the specimens was rapid initially, but decreased with time for a spherical void that contained little gas on the grain boundary, whereas only a little shrinkage was found for the spherical voids within grains during initial annealing.

The difference is caused by the opposite dependency of the gas-free void shrinkage process upon the void spacing on grain boundaries to that on the grain radius within grains. The healing time is approximately proportional to the void spacing[50] and inversely proportional to the grain size, as given above. That is, as the void shrinks, the relative void spacing and grain size to the void radius is enlarged, which either reduces or enhances the gradient of the chemical potential close to the void surface, and then either depresses or elevates finally the related rate of the void shrinkage, respectively.

Hence, it cannot be simply concluded that the shrinkage rate of the gas-free voids of identical radius within grains is positively lower than that on grain boundaries for α – Fe. The situation is similar even in copper,[17,20] whereas the diffusivity ratio of grain boundaries to lattices (D_{gb}/D_l) in iron is 10 times that in copper at the temperature interval involved. For the experimental observations in copper in which the rate of void shrinkage on grain boundaries was higher than that within grains,[17,20] the only appropriate explanation should be the inverse dependency of the void shrinkage process upon the half-void spacing on grain boundaries with that on the grain radius within grains at the initial shrinkage of the voids. The prediction also suggested[50] that the time to eliminate a spherical void with an identical radius within grains is close to that on grain boundaries at a fixed temperature, and is related to spherical void size, void spacing, and the grain size. Therefore, equivalent attention should be devoted to the shrinkage process of spherical voids within grains when that on grain boundaries is evaluated.

Most important, the predictions suggest that it is possible to wholly heal small micron-sized spherical voids in grains of pure iron within hours by annealing at high temperature. Moreover, the calculations also clarify that the times to heal spherical voids within grains are comparable with those on a grain boundary for pure iron at the temperature range selected. This means that the high-temperature annealing for the spherical void shrinkage can be carried out in practice wherever the void

is located (either within a grain or on a grain boundary). Actually, our corresponding experimental works in progress also showed that only spherical voids with the radii of $\rho_0 = 0.5 \sim 1.0$ can be observed both within grains and on grain boundaries for pure iron after the morphology evolutions of internal penny-shaped microcracks, which were fatigue induced, annealed at the temperature of 1173 K.

In addition, calculations revealed that the times to heal spherical voids were inversely proportional to the grain sizes, at the center of which the voids existed. These results suggest that the grain coarsening during the annealing at a high temperature could accelerate the spherical void shrinkage. It should also be noted that the hydrostatic pressure has no effect on the shrinkage process of the spherical void within grains, which greatly differs from the situation on grain boundaries. On the other hand, it is usually difficult to observe the void shrinkage process because of small size (<10 μm). The predictive modeling and theoretical analyses are thus beneficial in understanding the spherical void shrinkage.

Consequently, the total time can be accurately predicted to heal an internal penny-shaped microcrack, which was fatigue-induced, in a polycrystalline solid, on the basis of the model presented, and the proper relationship between the initial sizes of the spherical voids and the geometrical dimensions of the original internal microcrack, which evolved into the spherical voids. Furthermore, the annealing techniques can be correctly determined with appropriate parameters of temperatures and times to heal the internal microcracks with various geometrical dimensions, depending on the crystal lattices and grain sizes. In practice, the healing techniques can be applied to eliminate the internal microcracks in materials and to recover the properties of the materials, assuming the geometric dimensions of internal microcracks are available from equations for the crack growth.

5. Conclusions

A model is presented to describe a spherical void shrinkage within the center of a quasi-spherical grain dominated by the

Table 2 Total Time to Fully Heal Spherical Voids with a Radius of ρ_0

t_0 (h)		α – Fe			γ – Fe		
ρ_0 (μm)	R (μm)	973 K	1073 K	1173 K	1200 K	1300 K	1400 K
0.5	100	0.33	0.03		0.34	0.05	
	20	1.52	0.11		1.62	0.22	0.04
1.0	100	4.88	0.35	0.04	5.50	0.75	0.13
	20	23.2	1.65	0.18	25.8	3.64	0.63
1.5	100	24.1	1.80	0.20	26.7	3.61	0.62
	20	117	8.36	0.93	125	17.0	2.92
2.0	100	80.6	5.80	0.64		12.1	2.16
	20		27.4	2.80		49.2	8.48
2.5	100		13.0	1.50		27.6	5.35
	20		55.5	6.15			20.6
3.0	100		28.1	3.12			10.2
	20			13.2			45.1

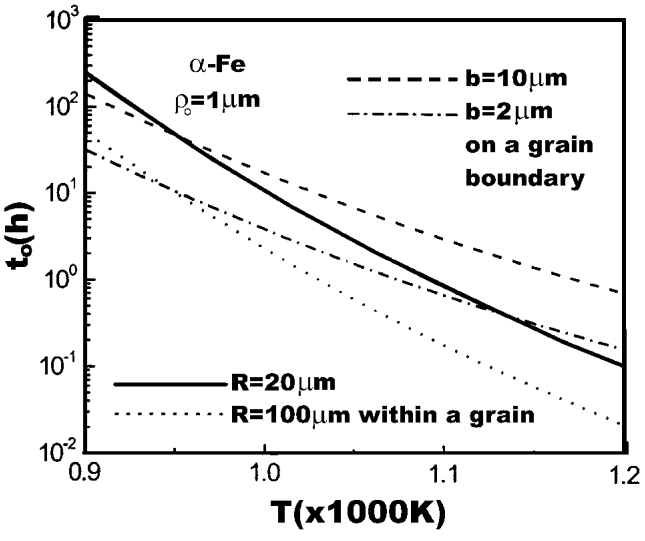

Fig. 10 Differences in the healing time as a function of temperature for a spherical void with an initial radius of $\rho_0 = 1$ μm between those within grain radii of $R = 20$ and 100 μm and with half-void spacing of $b = 2$ and 10 μm, on the grain boundary, respectively, in α – Fe

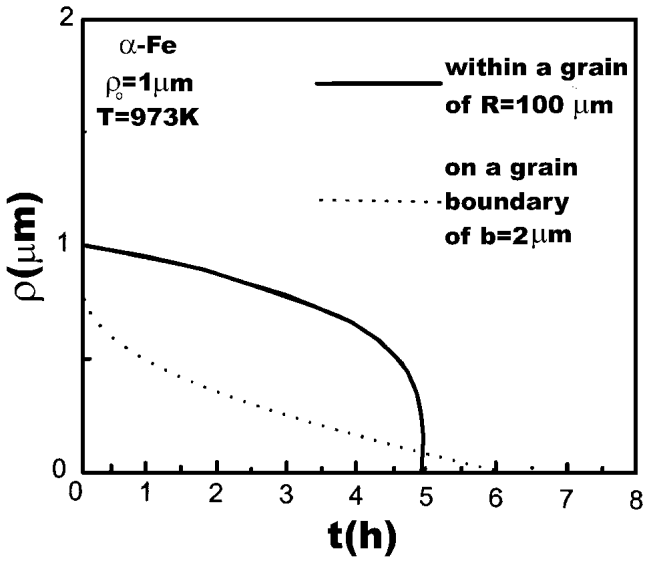

Fig. 11 Change in radius of a shrinking spherical void within a grain compared with that on a grain boundary interface as function of the annealing time for α – Fe

lattice self-diffusion based on the difference and the spherical symmetry distribution assumed in chemical potential between the spherical void surface and the grain boundary interface of the quasi-spherical grain. The quantitative predictions for a spherical void shrinkage within the center of a quasi-spherical grain in pure iron were completed. The main results obtained are summarized as follows:

- Only small micron-sized spherical voids could be totally healed within hours by annealing at an acceptable high temperature. The time to heal the spherical voids with identical ρ_0 highly depends on crystal lattice, temperature, and grain size, especially the initial radius of the void.
- The time to eliminate a spherical void with an identical radius within grains is close to that on grain boundaries at a fixed temperature, and is related to void size, void spacing, and the grain size.
- The times, $t_0(h)$, to heal a spherical void with an initial radius of ρ_0 are positively and linearly related to the values of ρ_0 with similar slopes of $n = 4$, i.e., $t_0(h) \propto \rho_0^4$, regardless of crystal lattices, grain sizes, and temperatures selected.
- The shrinkage of a spherical void is promoted by increasing the temperature, which elevates the diffusion coefficient. The shrinkage process of the spherical void in grains is also independent of an external hydrostatic pressure, which is different from the situation of the spherical void on a grain boundary interface.
- The healing time is approximately inversely proportional to the size of a grain surrounded by a spherical void with a radius of ρ_0, namely, $t_0 \propto 1/R$.

Acknowledgment

The author wishes to express his special thanks for the support of the National Outstanding Young Investigator Grant of China through Grant No. 59925104. The financial support from the National Natural Science Foundation of China under Grant 59889101 is also gratefully acknowledged. Valuable comments and kind suggestions from the reviewer also are sincerely appreciated.

References

1. T.K. Gupta: "Crack Healing in Thermally Shocked MgO," *J. Am. Ceram. Soc.,* 1975, *58,* pp. 143-48.
2. R. Dutton: "Comments on Crack Healing in UO_2," *J. Am. Ceram. Soc.,* 1973, *56,* pp. 660-61.
3. A.G. Evens and E.A. Charles: "Strength Recovery by Diffusive Crack Healing," *Acta Metall.,* 1977, *25,* pp. 919-27.
4. J. Rodel and A.M. Glaser: "High-Temperature Healing of Lithographically Introduced Cracks in Sapphire," *J. Am. Ceram. Soc.,* 1990, *73,* pp. 592-601.
5. J.D. Powers and A.M. Glaeser: "High-Temperature Healing of Crack-like Flaws in Mg- and Ca-Ion-Implanted Sapphire," *J. Am. Ceram. Soc.,* 1992, *75,* pp. 2547-58.
6. F. Yao, K. Ando K, and M.C. Chu: "Crack-Healing Behavior, High Temperature and Fatigue Strength of SiC-Reinforced Silicon Nitride Composite," *J. Mater. Sci. Lett.,* 2000, *19,* pp. 1081-85.
7. T.K. Gupta: "Instability of Cylindrical Voids in Alumina," *J. Am. Ceram. Soc.,* 1978, *61,* pp. 191-95.
8. W.C. Carter and A.M. Glaeser: "Dihedral Angle Effects on the Stability of Pore Channels," *J. Am. Ceram. Soc.,* 1984, *67,* pp. C-124-27.
9. M.D. Drory and A.M. Glaeser: "The Stability of Pore Channels: Experimental Observations," *J. Am. Ceram. Soc.,* 1985, *68,* pp. C-14-15.
10. Y. Takahashi, F. Ueno, and K. Nishiguchi: "A Numerical Analysis of the Void-Shrinkage Process Controlled by Surface-Diffusion," *Acta Metall.,* 1988, *36,* pp. 3007-18.
11. J. Pan and A.C.F. Cocks: "A Numerical Technique for the Analysis of Coupled Surface and Grain-Boundary Diffusion," *Acta Metall.,* 1995, *43,* pp. 1395-1406.
12. F.A. Nichols and W.W. Mullins: "Surface (Interface) and Volume-Diffusion Contributions to Morphological Changes Driven by Capillarity," *Trans. AIME,* 1965, *233,* pp. 1840-47.
13. F.A. Nichols and W W. Mullins: "Morphological Changes of Surface of Revolution Due to Capillarity-Induced Surface Diffusion," *J. Appl. Phys.,* 1965, *36,* pp. 1826-35.
14. F.A. Nichols: "On the Spheroidization of Rod-Shaped Particles of Finite Length," *J. Mater. Sci.,* 1976, *11,* pp. 1077-82.
15. P.Z. Huang, Z.H. Li, and J. Sun: "Finite Element Analysis of the Splitting and Cylinderization Processes of Damage Microcracks," *Modeling Simul. Mater. Sci. Eng.,* 2001, *9*(2), pp. 193-206.
16. W.C. Carter and A.M. Glaeser: "The Morphological Stability of Continuous Intergranular Phases: Thermodynamic Considerations," *Acta Metall.,* 1987, *35,* pp. 237-45.
17. A. Gittings: "The Stability of Grain Boundary Cavities in Copper," *Acta Metall.,* 1988, *16,* pp. 517-22.
18. G.K. Walker and H.E. Evans: "The Kinetics of the Annealing of High-Temperature Fracture Damage in a Stainless Steel," *Met. Sci. J.,* 1970, *4,* pp. 155-60.
19. H.E. Evans and G.K. Walker: "The Sintering of Cavities by Grain-Boundary Diffusion," *Met. Sci. J.,* 1970, *4,* pp. 210-12.
20. W.B. Beere and G.W. Greenwood: "The Effect of Hydrostatic Pressure on the Shrinkage of Cavities in Metals," *Met. Sci. J.,* 1971, *5,* pp. 107-13.
21. H.H. Yu and Z. Suo: "An Axisymmetric Model of Pore-Grain Boundary Separation," *J. Mech. Phys. Solids,* 1999, *47,* pp. 1131-41.
22. C.F. Yen and R.L. Coble: "Spheroidization of Tubular Voids in Al_2O_3 Crystals at High Temperatures," *J. Am. Ceram. Soc.,* 1972, *55,* pp. 507-509.
23. D.L. Smith and B. Evens: "Diffusional Crack Healing in Quartz," *J. Geophys. Res.,* 1984, *89,* pp. 4125-35.
24. Y. Takahashi, K. Takahashi, and K. Nishiguchi: "A Numerical Analysis of Void Shrinkage Processes Controlled by Coupled Surface and Interface Diffusion," *Acta Metall.,* 1991, *39,* pp. 3199-216.
25. Y. Takahashi, K. Inoue, and K. Nishiguchi: "Identification of Void Shrinkage Mechanisms," *Acta Metall.,* 1993, *41,* pp. 3077-84.
26. Y. Takahashi and K. Inoue: "Recent Void Shrinkage Models and Their Applicability to Diffusion Bonding," *Mater. Sci. Technol.,* 1992, *8,* pp. 953-64.
27. B. Derby and E.R. Wallach: "Theoretical Model for Diffusing Bonding," *Met. Sci.,* 1982, *16,* pp. 49-56.
28. E. Arzt, M.F. Ashby, and K.E. Easterling: "Practical Applications of Hot-Isostatic Pressing Diagrams-Four Case Studies," *Metall. Trans.,* 1983, *14A,* pp. 211-21.
29. A. Hill and E.R. Wallach: "Modeling Solid-State Diffusion Bonding," *Acta Metall.,* 1989, *37,* pp. 2425-37.
30. G.C. Kuczynski: "The Mechanism of Densification During Sintering of Metallic Particles," *Acta Metall.,* 1956, *4,* pp. 58-61.
31. M.F. Ashby: "A First Report on Sintering Diagrams," *Acta Metall.,* 1974, *22,* pp. 275-89.
32. Z.X. Guo and N. Ridley: "Modelling of Diffusion Bonding of Metals," *Mater. Sci. Technol.,* 1987, *3,* pp. 245-53.
33. D. Hull and D.E. Rimmer: "The Growth of Grain-Boundary Voids Under Stress," *Philos. Mag.,* 1959, *4,* pp. 673-87.
34. F.A. McClintock: "A Criterion for Ductile Fracture by the Growth of Holes," *J. Appl. Mech.,* 1968, *35,* pp. 363-71.
35. J.W. Hancock: "Creep Cavitation Without a Vacancy Flux," *Met. Sci.,* 1976, *10,* pp. 319-25.
36. T.-J. Chuang, K.I. Kagawa, J.R. Rice, and L.B. Sills: "Non-Equilibrium Models for Diffusive Cavitation of Grain Interfaces," *Acta Metall.,* 1979, *27,* pp. 265-84.
37. M.V. Speight and W. Beere: "Vacancy Potential and Void Growth on Grain Boundaries," *Met. Sci.,* 1975, *9,* pp. 190-91.
38. Q. Ma: "Non-linear Capillarity Shape Evolution of Rod Morphologies Via Interfacial Diffusion," *Acta Metall.,* 1998, *46,* pp. 1669-81.

39. L. Martinez and W.D. Nix: "A Numerical Study of Cavity Growth Controlled by Coupled Surface and Grain Boundary Diffusion," *Metall. Trans.,* 1982, *13A,* pp. 427-37.
40. C. Herring: "Diffusional Viscosity of a Polycrystalline Solid," *J. Appl. Phys.,* 1950, *21,* pp. 437-45.
41. C. Herring: *Physics of Powder Metallurgy,* W.E. Kingston, ed., McGraw-Hill Book, New York, 1951, p. 143.
42. W.D. Kingery and M. Berg: "Study of the Initial Stages of Sintering Solids by Viscous Flow, Evaporation-Condensation, and Self-Diffusion," *J. Appl. Phys.,* 1955, *26,* pp. 1205-11.
43. H.E. Exner and P. Bross: "Material Transport Rate and Stress Distribution During Grain Boundary Diffusion Driven by Surface Tension," *Acta Metall.,* 1979, *27,* pp. 1007-13.
44. S. Onaka and M. Kato: "Unified Analysis for Various Diffusion-Controlled Deformation and Fracture Process," *ISIJ Int.,* 1991, *31,* pp. 331-41.
45. J.K. Lee and T.H. Courney: "Two-Dimensional Finite Difference Analysis of Shape Instabilities in Plates," *Metall. Trans.,* 1989, *20A,* pp. 1385-94.
46. P.Z. Huang, Z.H. Li, and J. Sun: "Finite Element Analysis on Evolution Process for Damage Microcrack Healing," *Acta Mech. Sin.,* 2000, *16,* pp. 254-63.
47. F. Parhami, R.M. McMeeking, A.C.F. Cocks, and Z. Suo: "Model for the Sintering and Coarsening of Rows of Spherical Particles," *Mech. Mater.,* 1999, *31,* pp. 43-61.
48. J.W. Martin and R.D. Doberty: *Stability of Microstructure in Metallic System,* Cambridge University Press, New York, 1976, p. 178.
49. J.P. Hirth and J. Lothe: *Theory of Dislocation,* McGraw-Hill Book, New York, 1968, p. 485.
50. J. Sun: "Prediction to Spherical Void Shrinkage on Grain Boundary in Pure Iron," submitted to *Metall. Mater. Trans. A.*